

# Lithogeochemistry and geochronology of the subalkaline felsic plutonism that marks the end of the Paleoproterozoic orogeny in the Salvador–Esplanada belt, São Francisco craton (Salvador, state of Bahia, Brazil)

*Litogeocquímica e geocronologia do plutonismo félscio subalcalino que marca o final da orogenia Paleoproterozoica no cinturão Salvador–Esplanada, Cráton São Francisco (Salvador, Bahia, Brasil)*

Jailma Santos de Souza-Oliveira<sup>1,2\*</sup>, Jean-Jacques Peucat<sup>3</sup>,  
Johildo Salomão Figueiredo Barbosa<sup>2</sup>, Luiz César Correa-Gomes<sup>2</sup>,  
Simone Cerqueira Pereira Cruz<sup>2</sup>, Ângela Beatriz Menezes Leal<sup>2</sup>, Jean-Louis Paquette<sup>4</sup>

**ABSTRACT:** Studies conducted over the last decade concerning the rocks that underlie the municipality of Salvador have shown a complex geological history with a great diversity of medium- to high-grade metamorphic lithotypes, deformed in several phases and frequently cut by tabular mafic dykes and irregular granitic bodies. The latter, which were the subject of this study, frequently outcrop along the coastline of Salvador and are classified petrographically as monzo-syenogranites. They are classified as subalkaline and peraluminous according to their geochemical data, and stand out for being enriched in light rare earth elements and having a strong negative Europium (Eu) anomaly. These rocks are produced from anatetic melts or through the interaction of mantle-derived magmas with crustal materials. The negative values of  $\epsilon_{\text{Nd}(t)}$  (-6.08) corroborate with the crustal character and in the diagrams of tectonic ambience, they are plotted in the field of post-tectonic granites. The Sm-Nd model age ( $T_{\text{DM}}$ ) around 2.9 Ga indicates a neoarchean source for these lithotypes, whereas their U-Pb zircon age (LA-ICPMS) of  $2,064 \pm 36$  Ma is similar to the U-Pb (SHRIMP) and Pb-Pb (evaporation) ages for late-tectonic granites of the Itabuna–Curaçá–Salvador belt. Considering the results of recent studies in the area of Salvador, the monzo-syenogranites can be interpreted as late-tectonic intrusions, since they are affected by dextral shear zones correlated with the last stage of deformation registered in the granulites of Salvador.

**KEYWORDS:** monzo-syenogranites; petrology; geochronology; Salvador; Bahia; Brazil.

**RESUMO:** Estudos realizados ao longo da última década nas rochas que compõem o embasamento da cidade de Salvador, no nordeste do Brasil, mostram uma história geológica complexa, com grande diversidade de litotipos metamórficos de médio e alto grau, deformados de modo polifásico e frequentemente cortados por diques mafíticos tabulares e corpos graníticos irregulares. Estes últimos, objeto deste trabalho, afloram abundantemente na orla marítima de Salvador, sendo classificados petrograficamente como monzo-sienogranitos. Os seus dados geoquímicos permitem classificá-los como subalcalinos e peraluminosos, destacando-se que eles são enriquecidos em ETR leves e apresentam forte anomalia negativa de Eu. Estes granitóides apresentam características geoquímicas de rochas derivadas de material crustal e/ou produzidos pela interação de material da crosta e do manto, com os valores negativos de  $\epsilon_{\text{Nd}(t)}$  (-6,08) que corroboram a característica crustal. Em diagramas discriminantes de ambientes tectônicos, estão disponíveis no campo dos granitos pós-tectônicos. A idade-modelo Sm-Nd ( $T_{\text{DM}}$ ) em torno de 2,9 Ga indica uma fonte neoaqueana para esses litotipos enquanto que a idade U-Pb zircão (LA-ICPMS) de  $2,064 \pm 36$  Ma é interpretada como sendo de cristalização, sendo similar às idades U-Pb (SHRIMP) e Pb-Pb (evaporação) para os granitos tardí-tectônicos do Cinturão Itabuna–Salvador–Curaçá. Os monzo-sienogranitos em foco podem ser posicionados como granitos tardí-tectônicos, visto que são afetados por zonas de cisalhamento dextrais correlacionáveis com os estágios finais de deformação registrados nos granulitos de Salvador.

**PALAVRAS-CHAVES:** monzo-sienogranitos; petrologia; geocronologia; Salvador; Bahia; Brasil.

<sup>1</sup>Program for Post-Graduation in Geology, Universidade Federal da Bahia - UFBA, Salvador (BA), Brazil. E-mail: jailmasouza@gmail.com

<sup>2</sup>Basic Geology Nucleus, Institute of Geosciences, Universidade Federal da Bahia - UFBA, Salvador (BA), Brazil. E-mail: johildo@cpgg.ufba.br; lccgomes@gmail.com; simonencruzufba@gmail.com; angelab@ufba.br

<sup>3</sup>Institute of Geosciences, University of Rennes 1, 35042 Rennes Cedex, France. E-mail: jean-jacques.peucat@univ-rennes1.fr

<sup>4</sup>Laboratoire Magmas et Volcans, Département de Géologie, OPGC e Université Blaise Pascal. E-mail: J.L.paquette@opgc.univ-bpclermont.fr

\*Corresponding author

Manuscrito ID: 30105. Recebido em: 09/04/2014. Aprovado em: 14/05/2014.

## INTRODUCTION

The relationships between magmatic bodies and deformational events are useful to unravel the complex interactions between tectonics and the processes of generation and emplacement of magmas. Thus, granitoid bodies are good tracers of the rheological evolution of host rocks, as well as of stress fields and kinematics (Druguet *et al.* 2008). These rocks are present in different crustal levels at various scales, from large granitic plutons to small anatetic granitic veins (leucosome) in migmatitic terrains.

The granulitic rocks that outcrop in Salvador, state of Bahia, Brazil, are located nearby the confluence of two important tectonic macro-units of the São Francisco craton (SFC; Almeida 1977): the first one, with N45° trends, corresponds to the Salvador–Esplanada belt (SEB) of Barbosa and Dominguez (1996), and the second one, oriented N10°, corresponds to the Itabuna–Salvador–Curaçá belt (ISCB) of Barbosa and Sabaté (2002, 2004) (Fig. 1). Both units show a complex evolutionary history (Barbosa and Dominguez 1996, Barbosa and Sabaté 2002, 2004, Delgado *et al.* 2002), which makes it difficult to establish precise geotectonic models and the connection between these two units. The granitoids that occur in the ISCB can be classified as (i) syntectonic, contemporary to the formation of the belt and to the crustal thickening (~2.1 Ga), and (ii) post-tectonic, associated to sinistral transcurrent faults related to the peak of granulitic metamorphism and orogenic collapse (~2.07 Ga) (Barbosa *et al.* 2008).

This study had the objective of placing the granitic bodies and veins that outcrop in Salvador within the regional tectonic context. In addition, the petrographic, petrochemical, geochronological, and isotopic data of these rocks are presented and discussed, aiming to contribute to the knowledge of their tectonic environment.

## ANALYTICAL PROCEDURES

Twelve whole-rock granite analyses of major and trace elements were carried out at the laboratories of GEOSOL and Geology and Surveying Ltd., and are reported in Tab. 2. Major ( $\text{SiO}_2$ ,  $\text{Al}_2\text{O}_3$ ,  $\text{FeO}$  (t),  $\text{MgO}$ ,  $\text{CaO}$ ,  $\text{TiO}_2$ ,  $\text{P}_2\text{O}_5$ , and  $\text{MnO}$ ) and trace (V, Rb, Ba, Sr, Ga, Nb, Zr, Y, and Th) elements were analyzed by X-ray fluorescence, and rare earth elements were determined using inductively coupled plasma mass spectrometry (ICP-MS).  $\text{Na}_2\text{O}$  and  $\text{K}_2\text{O}$  contents were determined using atomic absorption spectrometry.

The procedures described by Peucat *et al.* (1999) were followed to analyze the Nd whole-rock isotopic compositions.

The values were adjusted to the pattern of Nd AMES standard, which provided a mean  $^{143}\text{Nd}/^{144}\text{Nd}$  ratio of  $0.511896 \pm 7$ , with an error of 0.0015%. The model ages ( $T_{\text{DM}}$ ) were calculated using values of  $\epsilon_{\text{Nd}} + 10$  for the current depleted mantle and  $^{147}\text{Sm}/^{144}\text{Nd}$  ratio of 0.2137, assuming a radiogenic linear growth starting at 4.54 Ga.

Several U-Pb (zircon) analyses were carried out for the monzo-syenogranite sample SG-10G at the Laboratoire Magmas et Volcans – Université Blaise Pascal in Clermont-Ferrand, France, using the *in situ* laser ablation inductively coupled plasma mass spectrometry (LA-ICPMS) method as described by Hurai *et al.* (2010). The error measured for each analysis (ratios and ages) is presented at the level of  $1\sigma$ . For the calculation of  $^{207}\text{Pb}/^{206}\text{Pb}$  weighted mean ages, a confidence limit of 95% was considered. The errors in the discordant intercept ages are presented at the level of  $2\sigma$  and were calculated using the software Isoplot (Ludwig 2001).

The  $^{207}\text{Pb}/^{206}\text{Pb}$  dating method through evaporation of lead from zircon monocrystals, developed by Kober (1986), was used for the same SG-10G sample by means of successive heating stages in a thermal ionization mass spectrometer (TIMS), using the Finnigan MAT 262 mass spectrometer of the Laboratoire de Géosciences Rennes-CNRS, France.

All ages were calculated using decay constants and abundance of the isotopes listed by Steiger and Jäger (1977).

## REGIONAL GEOLOGICAL SETTING

In the portion of the SFC that outcrops in the state of Bahia, high-grade metamorphic rocks occur in the area of Itabuna–Ilhéus, in the south, and in the area of Curaçá, in the north, comprising the Itabuna–Salvador–Curaçá block (ISCB) of Barbosa and Sabaté (2002, 2004). These rocks, at the current level of erosion, are the roots of an orogenic belt, with N-S orientation and Paleoproterozoic age of around 2.1 Ga (Peucat *et al.* 2011) (Fig. 1A). The southern part of this belt consists of at least four groups of tonalite/trondhjemite, three of them with Archean ages between 2.6 and 2.7 Ga (Peucat *et al.* 2011), and one Paleoproterozoic group (~2.2 Ga) (Barbosa and Sabaté 2004, Peucat *et al.* 2011) (Tab. 1). Subordinately, charnockitic bodies of Archean age also occur, as well as bands of supracrustal rocks and gabbros, and basalts related to ocean floor or back-arc basins (Teixeira 1997). In addition, intrusions of granulitized monzogranites of shoshonitic affinity are also found (Barbosa 1990). The northern area of the ISCB essentially consists of tonalite–trondhjemite–granodiorite (TTG) orthogneisses of 2.7 Ga (Figueiredo 1989,

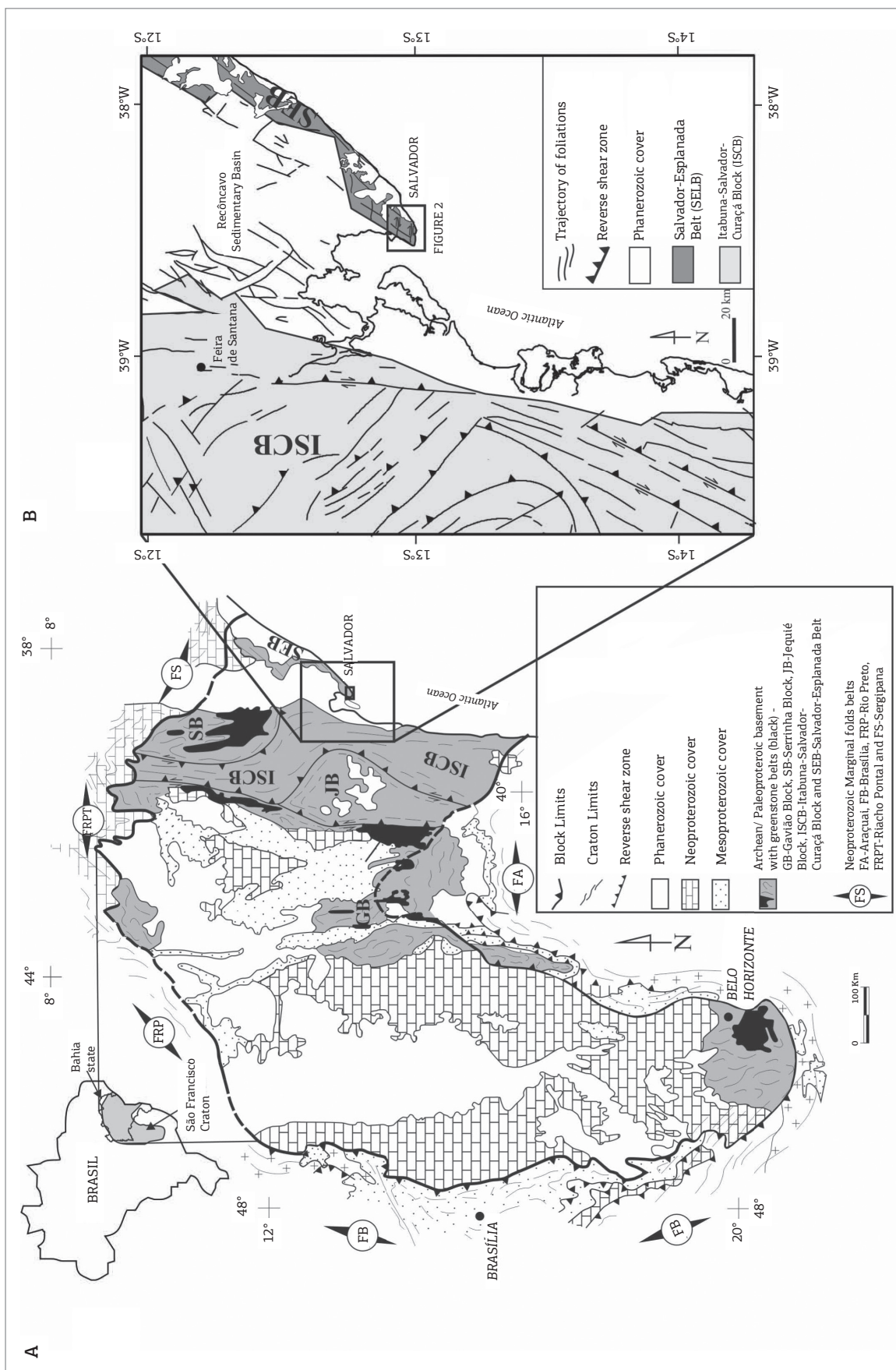


Figure 1. (A) São Francisco craton with the main tectonic units of its basement and the mobile belts of Neoproterozoic age (adapted from Alkmim *et al.* 1993). (B) Simplified geological map of the area where Salvador is located, showing the main geotectonic units (adapted from Dalton de Souza *et al.* 2003). The square near Salvador corresponds to the location of Fig. 2.

Table 1. U-Pb and Pb-Pb (zircon) ages of the Itabuna-Salvador-Curaçá block and of the Salvador-Esplanada belt (modified from Peucat *et al.* 2011)

Tectonic Unit	Rock	Magmatic zircon age (in heritage)	Metamorphic age in Ma	Methodology	Reference
Southern Itabuna-Salvador-Curaçá block	Shoshonite	2,075 ± 16 Ma	-	TIMS evap.	Ledru <i>et al.</i> (1994)
	Syenite of São Félix	2,098 ± 1	-	TIMS evap.	Rosa <i>et al.</i> (2001)
	Charno-enderbite (TT1)	2,092 ± 6	-	SHRIMP	Silva <i>et al.</i> (2002)
	Enderbite (TT1)	2,109 ± 19	2,081 ± 16	LA-ICPMS	Peucat <i>et al.</i> (2011)
	Tonalite	2,124 ± 10	-	SHRIMP	Silva <i>et al.</i> (2002)
	Enderbite (TT1)	2,131 ± 5	2,069 ± 19	SHRIMP	Silva <i>et al.</i> (2002)
	TT1	ca. 2.18 Ga	2,078 ± 13	LA-ICPMS	Peucat <i>et al.</i> (2011)
	TT1	2,191 ± 10	2,109 ± 17	SHRIMP	Peucat <i>et al.</i> (2011)
	Charno-enderbite	ca. 2.5 Ga	2,086 ± 36	TIMS evap.	Ledru <i>et al.</i> (1994)
	Enderbite of Ipiaú	2,634 ± 14	-	TIMS evap.	Ledru <i>et al.</i> (1994)
	Enderbite (TT2)	2,675 ± 11	2,080 ± 21	LA-ICPMS	Peucat <i>et al.</i> (2011)
	Enderbite (TT2-TT5)	2,719 ± 10	-	SHRIMP	Silva <i>et al.</i> (2002)
	Charno-enderbite	ca. 2.85 Ga	2,078 ± 20	SHRIMP	Silva <i>et al.</i> (2002)
Central Itabuna-Salvador-Curaçá block	TT5	ca. 2.7 and 2.9 Ga	2,098 ± 11	SHRIMP	Peucat <i>et al.</i> (2011)
	Granite (Bravo)	2,063 ± 6		SHRIMP	Barbosa <i>et al.</i> (2008)
	Charnockite (Tanquinho)	2,096 ± 3	-	TIMS evap.	Barbosa <i>et al.</i> (2008)
	Enderbite (Bravo)	2,070 ± 3	-	SHRIMP	Barbosa <i>et al.</i> (2008)
	Charnockite (Jacuípe/C. Nova)	2,126 ± 19	2,082 ± 7	SHRIMP	Silva <i>et al.</i> (1997)
	Leucogabbro (Jacuípe)	2,584 ± 8	2,082 ± 17	SHRIMP	Oliveira <i>et al.</i> (2010)
	Charnockite (Jacuípe)	2,634 ± 19 Ma (3.3 Ga)	2,072 ± 22	SHRIMP	Silva <i>et al.</i> 1997
	Opx tonalite (Jacuípe)	2,695 ± 12 Ma	2,072 ± 15	SHRIMP	Silva <i>et al.</i> 1997
Northern Itabuna-Salvador-Curaçá block	Enderbite (Riachão de Jacuípe)	ca. 2.2 (ca. 2.8 Ga)	2,028 ± 13	SHRIMP	Silva <i>et al.</i> (2002)
	Itiuba syenite	2,084 ± 9		SHRIMP	Oliveira <i>et al.</i> (2004)
	Itiuba syenite	2,095 ± 5		TIMS evap.	Conceição <i>et al.</i> (2003)
	Gabbro-norite (Medrado)	2,085 ± 5		SHRIMP	Oliveira <i>et al.</i> (2004)
	Norite (Caraíba)	2,580 ± 10	2,103 ± 23	SHRIMP	Oliveira <i>et al.</i> (2004)
	Amphibolite (Caraíba)	2,577 ± 110	2,083 ± 4	TIMS	D'el-Rey Silva <i>et al.</i> (2007)
Salvador-Esplanada belt	Tonalite	2,574 ± 6	2,074 ± 14	SHRIMP	Oliveira <i>et al.</i> (2010)
	Orthogneiss (Conde)	2,169 ± 48 (discordant)	-	SHRIMP	Silva <i>et al.</i> (2002)
	Granodiorite (Aporá)	2,954 ± 25	-	SHRIMP	Silva <i>et al.</i> (2002)
	Enderbite (Salvador)	2,561 ± 7	2,089 ± 11	SHRIMP	Silva <i>et al.</i> (1997)
	Granite (Salvador)	2,064 ± 36	-	LA-ICPMS	This work

Silva *et al.* 1997) (Tab. 1), with interbedded aluminous gneisses, calc-silicate rocks, metacarbonates, and quartzites (Melo *et al.* 1995), as well as mafic-ultramafic rocks that form the so-called São José do Jacuípe Suite, also of Archean age (Silva *et al.* 1997). The whole ISCB is intruded by syenites dated at 2.08 – 2.09 Ga (Conceição *et al.* 2003, Oliveira *et al.* 2004), and syn- and post-tectonic granites intrusions dated around 2.06 Ga (Silva *et al.* 2002, Barbosa *et al.* 2008). This entire crustal segment was strongly affected by Paleoproterozoic tectonics with all its lithotypes plunged into granulite facies metamorphism (Barbosa & Sabaté 2002, 2004).

The SEB of Barbosa and Dominguez (1996) consists of high-grade metamorphic rocks, which are roughly N45° aligned (Fig. 1B). These lithotypes underlie Salvador, in Bahia, and extend up to Boquim, in the state of Sergipe. A large portion of the northeastern part of the belt is covered by Tertiary deposits of the Barreiras Formation and, by Quaternary sediments, and in the southwestern part, by the sedimentary rocks of the Recôncavo-Tucano Mesozoic basin.

The SEB consists of migmatitic orthogneisses of alkali-line to subalkaline affinity, and tonalitic, charnoenderbitic, and charnockitic orthogneisses with calc-alkaline affinity. There are also orthogneisses with felsic tonalitic-granodioritic terms of 2.9 Ga (Silva *et al.* 2002) (Tab. 1), as well as amphibolized gabbros with tholeiitic affiliation and granites with alkaline tendency (Delgado *et al.* 2002).

In the region of Salvador, these rocks are plunged into granulite facies (Fujimori & Allard 1966, Fujimori 1968, 1988, Barbosa *et al.* 2005, Souza *et al.* 2010, among others), although northwards, according to Oliveira Júnior (1990), granulitic rocks grade to rocks of the amphibolite facies. These are cut by mafic dyke swarms (Mestrinho *et al.* 1988, Corrêa-Gomes *et al.* 1996, Menezes Leal *et al.* 2012) and by the granitic bodies (Celino *et al.* 1984), which have motivated this study.

Geologically, the area of Salvador (Fig. 2) was subdivided by Barbosa and Dominguez (1996) into three major domains: (i) the Alto de Salvador, which is a horst of granulitic rocks (Barbosa *et al.* 2005); (ii) the Recôncavo sedimentary basin, which is limited, eastwards, by the Salvador

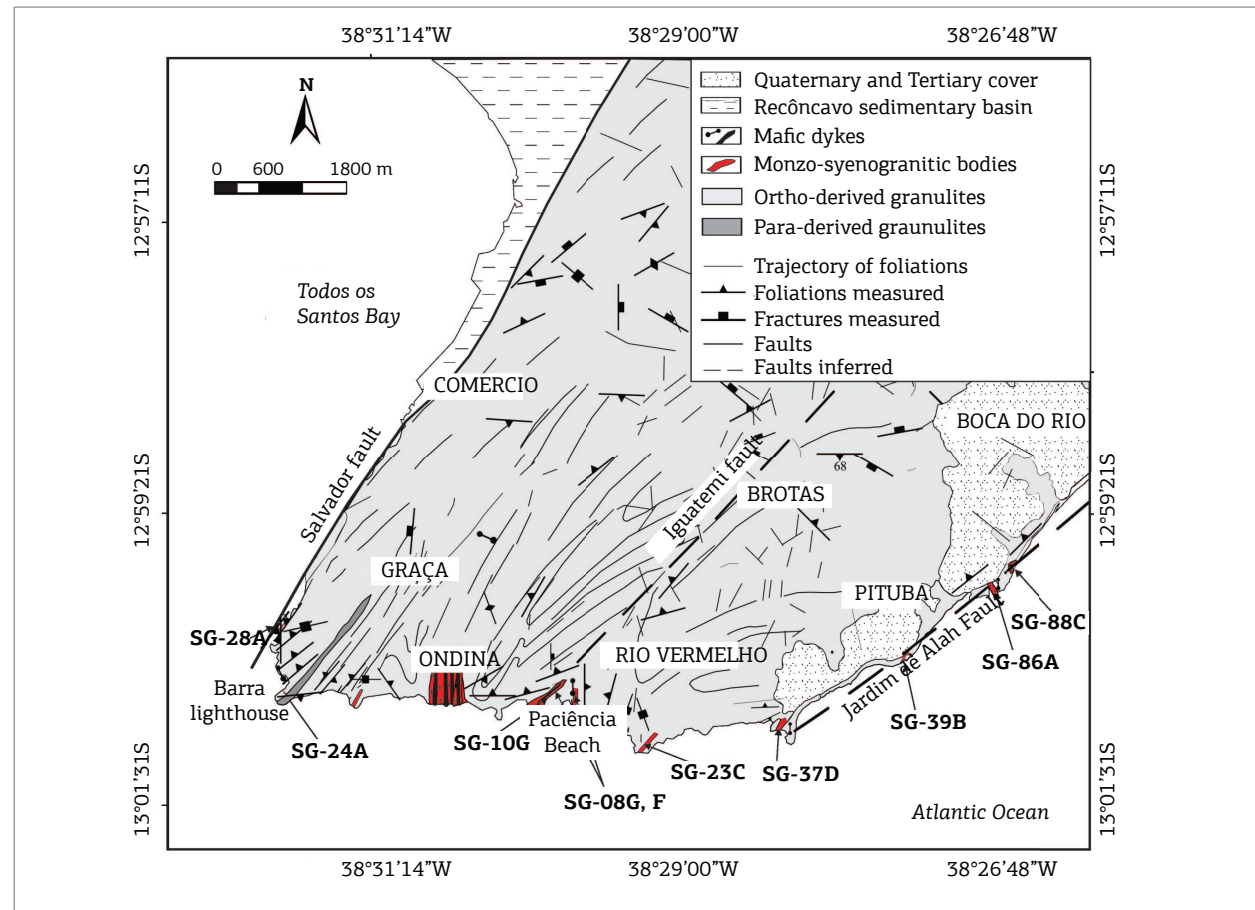


Figure 2. Simplified geological map of the area with the location of the studied samples.

Table 2. Chemical analyses of the rock samples of monzo-syenogranitic bodies and veins of Salvador

	<b>SG-37D</b>	<b>SG-28A</b>	<b>SG-36</b>	<b>SG-39B</b>	<b>SG-86A</b>	<b>SG-08G</b>	<b>SG-88C</b>	<b>SG-23C</b>	<b>SG-24A</b>	<b>SG-08F</b>
<b>SiO<sub>2</sub></b>	69.10	69.40	69.40	70.10	70.10	70.40	71.10	71.70	72.20	73.50
<b>TiO<sub>2</sub></b>	0.61	0.12	0.73	0.73	0.56	0.60	0.55	0.23	0.33	0.23
<b>Al<sub>2</sub>O<sub>3</sub></b>	14.50	15.10	14.70	14.00	14.20	13.40	14.10	13.40	13.60	13.10
<b>Fe<sub>2</sub>O<sub>3</sub></b>	0.91	2.10	0.92	0.26	1.70	0.81	1.70	2.00	0.96	0.01
<b>FeO</b>	4.20	0.86	3.50	4.60	2.00	3.00	2.27	2.20	2.60	1.70
<b>MnO</b>	0.04	.03	0.04	0.07	0.03	0.03	0.03	0.03	0.04	0.02
<b>MgO</b>	1.00	0.55	1.20	0.81	0.70	0.81	0.64	0.72	0.63	0.56
<b>CaO</b>	1.90	0.70	0.63	1.80	1.10	1.60	1.40	0.61	1.20	0.40
<b>Na<sub>2</sub>O</b>	2.20	2.30	2.00	2.60	1.80	2.20	2.30	1.70	2.00	1.60
<b>K<sub>2</sub>O</b>	6.10	8.00	6.50	6.00	7.10	6.30	7.10	8.00	6.00	7.80
<b>P<sub>2</sub>O<sub>5</sub></b>	0.18	0.06	0.18	0.23	0.16	0.20	0.16	0.03	0.08	0.14
<b>PF</b>		0.18				0.19			0.14	0.59
<b>Total</b>	100.74	99.22	99.80	100.20	99.45	99.35	100.35	100.62	99.64	99.06
<b>V</b>	39	16	41	46	59	37	44	8	19	8
<b>Rb</b>	195	164	206	162	217	213	173	333	284	335
<b>Ba</b>	1.310	3.729	1.419	1.590	1.333	1.468	1.328	943	611	988
<b>Sr</b>	266	636	285	293	386	392	313	186	133	271
<b>Nb</b>	19	<5	11	13	15	58		18	38	25
<b>Zr</b>	820	323	829	859	979	786	853	211	407	417
<b>Y</b>	85	11	45	62	54	39	47	36	60	48
<b>Th</b>	< 5	< 5	< 5	< 5	6.3	29	7.6	113	68	55
<b>La</b>	134.79	22.48	50.95	49.91	66.10	178.90	83.50	221.00	140.27	209.20
<b>Ce</b>	229.31	30.01	115.88	97.81	120.00	324.50	157.00	378.50	273.40	394.30
<b>Nd</b>	50.36	7.78	40.45	39.18	57.60	103.90	68.80	159.00	106.80	131.90
<b>Sm</b>	6.90	1.21	6.77	7.68	9.40	17.57	10.90	18.37	18.33	20.52
<b>Eu</b>	0.18	1.29	0.63	1.05	1.93	2.33	2.23	2.14	1.40	1.83
<b>Gd</b>	3.94	0.98	4.58	6.07	8.54	10.04	8.90	11.50	13.13	11.22
<b>Dy</b>	1.51	0.47	1.46	2.47	5.24	5.31	5.06	5.09	7.07	4.92
<b>Ho</b>	0.29	0.10	0.26	0.01	0.98	1.08	1.02	0.96	1.19	0.88
<b>Er</b>	0.76	0.30	0.52	1.10	2.68	2.28	2.78	2.19	2.03	1.89
<b>Yb</b>	0.31	0.29	0.53	0.76	2.60	1.44	2.40	1.33	1.13	1.11
<b>Lu</b>	0.03	0.06	0.09	0.16	0.38	0.24	0.36	0.14	0.14	0.20

fault system; and (iii) the Atlantic Coastal Margin, composed of Tertiary and Quaternary deposits of unconsolidated sediments (Dominguez *et al.* 1999).

Despite the lack of outcrops, the studies carried out by Barbosa *et al.* (2005), focusing on the western area of the horst, showed a great diversity of ortho- and para-derived metamorphic lithotypes of high- and medium-metamorphic grade, which are polydeformed and frequently cut by mafic dykes and irregular monzo-syenogranitic bodies. Souza *et al.* (2010 and references therein) grouped these rocks into four units: (i) the predominant ortho-derived granulites, with granulitized ultramafic and mafic enclaves; (ii) the para-derived granulites; (iii) the monzo-syenogranitic bodies and veins; and (iv) the mafic dykes (Fig. 2).

Regarding the ductile deformations, at least three stages of continuous deformation were recorded by Barbosa *et al.* (2005) on the granulitic lithotypes, which are the host rocks of the monzo-syenogranitic bodies and veins in question. The main structures of the first stage comprised recumbent folds with subhorizontal axes, which were isoclinally refolded during the second phase. These isoclinal folds have subvertical axial planes and subhorizontal axes. The third phase includes transcurrent dextral shear zones, subparallel to the axial surfaces of the isoclinal folds, which are coeval with the second deformational phase and produce mineral stretching lineations parallel to their axes. U-Pb monazite ages (*in situ* LA-ICPMS) indicate that the third deformational phase occurred at  $2,064 \pm 9$  Ma (Souza 2013).

Numerous faults and fractures cut the granulitic rocks. The most significant are those oriented N60° – N90°, associated with the intrusion of mafic dykes, and those oriented N120° – N160°, where tabular bodies and monzo-syenogranitic veins were placed. In addition to these, faults oriented N30° have also been registered, and the Iguatemi and Jardim de Alah faults (Fig. 2) exhibit a general N40° orientation.

Although Souza *et al.* (2010 and references therein) recently presented important results on the granulitic rocks, various geological problems still need to be solved. One of them, which shows the generation and age of the felsic magmatism of the SEB, will be dealt with in this study.

## PETROGRAPHICAL AND GEOCHEMICAL ASPECTS

The monzo-syenogranitic dykes and veins outcropping along the coast of Salvador (Fig. 2) fill fractures in various directions. Two dominant directions present are as follows:

1. Fractures oriented N60° – N90°: The dykes exhibit fine- to medium-grained texture, are moderately deformed,

and present folds and boudinage when affected by the late dextral shear zones correlated to the third stage of deformation of Barbosa *et al.* (2005). Mafic dykes were observed with the same orientation. In the outcrop of the Paciência Beach (SG-10F) for example, interpenetrations of mafic material in felsic material and vice versa were identified, characterizing a mingling-type heterogeneous physical mixing of basaltic and granitic magma (Walker & Skelhorn 1966, Wiebe 1991) (Figs. 3A and B).

2. Fractures oriented N40° – N70°: The dykes present medium- to coarse-grained texture and occur as vertical and subvertical bodies, with thickness ranging from 0.5 to 2 m and keeping abrupt contacts with their host rocks (Fig. 3C). Irregular bodies are also found, with various thicknesses and diffuse contacts. On the edge of some of the granitoid dykes, in contact with the host rocks, pegmatitic facies were observed, probably related to late magmatic-hydrothermal processes.

From a petrographic point of view, these felsic bodies and veins are classified as monzo-syenogranites. They show quartz (30 – 40%), microcline (30 – 40%), biotite (15%), and plagioclase (5 – 10%) as major minerals. Apatite, opaque minerals, and zircon occur as accessory minerals.

The geochemical data of the major elements allowed classifying them as subalkaline and peraluminous (Fig. 4A and B), characterizing their origin as formed by the partial fusion of a crustal source (Chappell & White 1974, White & Chappell 1977). They are acidic rocks, with SiO<sub>2</sub> contents ranging from 69 to 73% (Tab. 2). The Harker (1909) type binary diagrams show magmatic differentiation trends, in which TiO<sub>2</sub>, Na<sub>2</sub>O, MgO, Sr, Zr, and Ba are compatible with fractional crystallization whereas K<sub>2</sub>O and Rb are incompatible (Fig. 5). Furthermore, as shown in Fig. 6, these lithotypes are enriched in light rare earth elements (LREE) ( $136 < La_N < 602$ ) and present a strong negative Europium (Eu) anomaly. The geochemical data of their trace elements, represented in discrimination diagrams of tectonic environment, are not conclusive. Most of them are located in the fields of intraplate and syncollision granites of Pearce *et al.* (1984), but some samples plot in the field of post-collision granites of Pearce (1996) (Figs. 7A and 7B).

## ISOTOPIC GEOCHEMISTRY AND GEOCHRONOLOGY

The SG-10G sample of a monzo-syenogranite vein corresponds to a representative part of the felsic portion of the mingling-type mixture observed at Paciência Beach (Fig. 3B).

One sample (SG-10G) of the monzo-syenogranitic bodies was selected for U-Pb zircon dating. This sample was intrusive into the ortho-derived granulites, at the Rio Vermelho district in the city of Salvador (Figs. 2 and 3). Dated zircon grains are large (spot size in Fig. 8 is *ca.* 30 µm) and they are mainly clear, euhedral, elongated, and without any visible inherited core (see TL images of grains 1.1 and 2.1 in Fig. 8). They are typical of high-temperature types (S19-S24, Fig. 8, after Pupin (1980)). The protolith of these granulites were dated at 2,561 ± 7 Ma and the granulite facies were 2,089

± 11 Ma by U-Pb sensitive high-resolution ion microprobe (SHRIMP) zircon ages (Silva *et al.* 1997).

U-Pb zircon ages obtained using ICP-MS data are concordant to slightly discordant and define an intercept age at 2,064 ± 36 Ma, with the mean of  $^{207}\text{Pb}/^{206}\text{Pb}$  ages of 2,067 ± 13 Ma in 21 analyses. These ages are similar to the Pb-Pb zircon TIMS evaporation age also obtained in this study (*i.e.*, 2,064 ± 6 Ma) and are interpreted as the age of crystallization of the granites. Three grains that exhibit zoned cores (see grains 8.1 and 19.1 in Fig. 8) showed  $^{207}\text{Pb}/^{206}\text{Pb}$

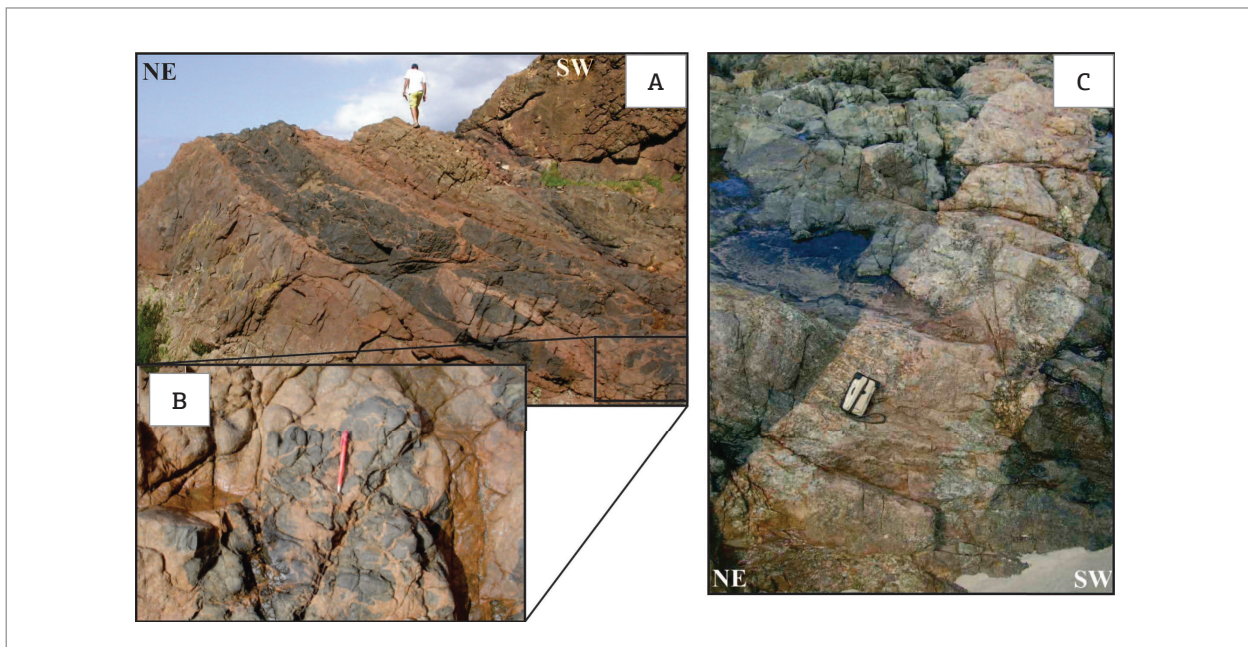


**Figure 3.** Association of the monzo-syenogranitic veins with mafic dykes in fractures and faults with orientation of N60° – N90°. (A) Panoramic view of Paciência Beach. (B) Detail of a physical mixing of basaltic and granitic magma (mingling). (C) Verticalized monzo-syenogranitic body with pegmatoid texture and abrupt contacts with its host rocks.

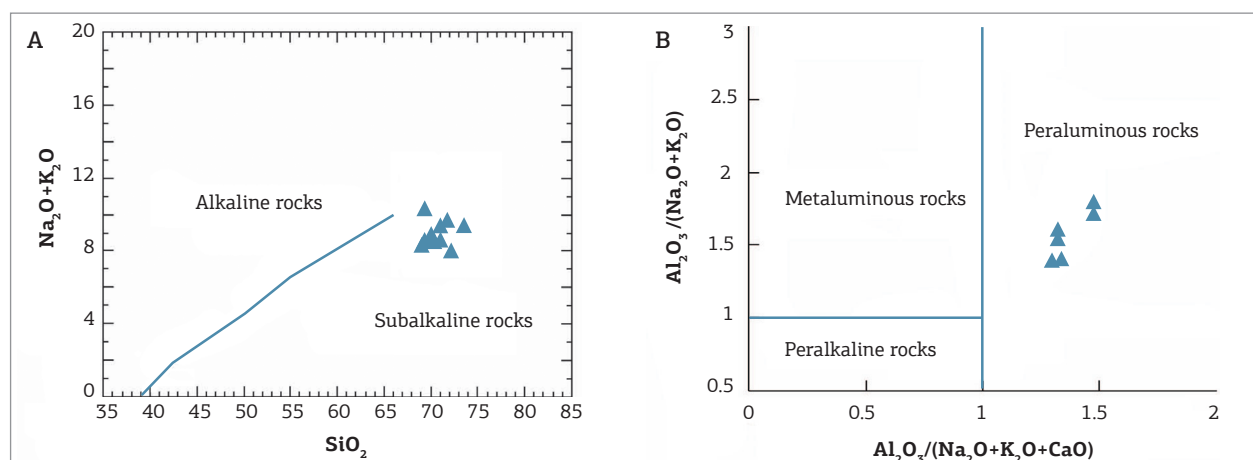


**Figure 4.** (A) The  $(\text{Na}_2\text{O} + \text{K}_2\text{O})$  versus  $\text{SiO}_2$  diagram of Irvine and Baragar (1971), showing the subalkalinity of the monzo-syenogranitic bodies of Salvador. (B) The  $\text{Al}_2\text{O}_3/(\text{Na}_2\text{O} + \text{K}_2\text{O})$  versus  $\text{Al}_2\text{O}_3/(\text{Na}_2\text{O} + \text{K}_2\text{O} + \text{CaO})$  diagram of Shand (1950), characterizing their peraluminous character.

ages of *ca.* 2.3 – 2.4 Ga, which were interpreted as an inheritance from the surrounding Archean basement.

Whole-rock Sm-Nd elemental and isotopic data obtained from the same sample were as follows: Sm = 22.9219 ppm; Nd = 134.6957 ppm;  $^{147}\text{Sm}/^{144}\text{Nd} = 0.1028$ ;  $^{143}\text{Nd}/^{144}\text{Nd} = 0.5110$ . These data provided a model age ( $T_{\text{DM}}$ ) of 2.859 Ga, and  $\epsilon_{\text{Nd}(0)} = -30.9$ . Considering the 2.07 Ga crystallization age, the parameter  $\epsilon_{\text{Nd}(2.07\text{Ga})}$  results in the value of -6.08, suggesting an important

participation of a crustal component in the formation of these granites.

## DISCUSSIONS AND CONCLUSIONS

The data obtained in this study from the monzo-syenogranitic bodies and veins intrusive into the granulites of Salvador allow us to classify them as subalkaline

**Table 3.** U-Pb zircon LA-ICPMS analyses of the SG-10G monzo-syenogranitic vein sample of the municipality of Salvador

Spot	U (ppm)	Th (ppm)	Pb (ppm)	Th/U	Radiogenic Ratios				Age (Ma)			
					$^{207}\text{Pb}/^{235}\text{U}$	2 σ	$^{206}\text{Pb}/^{238}\text{U}$	2 σ	Rho	$^{207}\text{Pb}/^{206}\text{Pb}$	2 σ	% Conf.
1.1	289	189	105	0.65	6.74422	0.24760	0.38040	0.00772	0.55	2,067	46	99.5
2.1	185	98	63	0.53	6.56174	0.25392	0.36814	0.00752	0.53	2,054	47	97.0
3.1	53	35	19	0.66	6.26562	0.48888	0.34072	0.00812	0.31	2,123	65	90.0
4.1	226	141	82	0.62	6.22636	0.25570	0.35932	0.00740	0.50	2,061	48	95.4
5.1	185	163	68	0.88	6.65582	0.27588	0.37035	0.00762	0.50	2,056	48	97.3
6.1	75	89	26	1.19	5.74885	0.32160	0.33724	0.00734	0.39	2,062	55	90.4
7.1	169	91	60	0.54	6.61456	0.26610	0.37814	0.00776	0.51	2,066	48	99.2
8.1*	560	445	213	0.79	8.36682	0.32458	0.38075	0.00778	0.53	2,437	46	84.6
9.1	161	84	57	0.52	6.25340	0.26074	0.36558	0.00754	0.49	2,037	50	99.3
10.1	57	51	22	0.91	6.54712	0.33326	0.38979	0.00826	0.42	2,066	53	97.5
11.1	221	117	66	0.53	6.67809	0.28180	0.37768	0.00780	0.49	2,094	50	86.7
12.1	705	645	230	0.91	6.11791	0.24444	0.32341	0.00664	0.51	2,162	49	83.1
13.1	151	207	54	1.37	6.44963	0.27900	0.36437	0.00754	0.48	2,079	50	98.2
14.1	81	103	33	1.27	6.66357	0.32334	0.37270	0.00784	0.43	2,049	53	97.8
15.1	167	136	60	0.81	6.26328	0.28008	0.35151	0.00732	0.47	2,051	52	90.2
16.1	149	123	48	0.83	5.89366	0.29892	0.33694	0.00718	0.42	2,045	55	90.1
17.1	62	115	32	1.86	8.43920	0.43292	0.42482	0.00900	0.41	2,294	52	97.7
18.1	35	65	15	1.84	5.65214	0.39850	0.35236	0.00814	0.33	2,045	65	94.1
19.1*	169	64	83	0.38	8.97502	0.45172	0.41770	0.00886	0.42	2,387	52	100.2
20.1	160	119	47	0.74	5.30388	0.31966	0.29336	0.00654	0.37	2,059	61	83.9
21.1	126	67	43	0.53	6.49940	0.30520	0.36499	0.00766	0.45	2,083	54	94.8
22.1	68	68	27	1.00	5.82315	0.34050	0.34214	0.00752	0.38	2,053	59	92.1
23.1	1,252	153	330	0.12	5.25620	0.23316	0.30106	0.00628	0.47	2,044	53	84.9
24.1	254	166	91	0.66	6.50761	0.28556	0.37321	0.00774	0.47	2,049	53	99.4

(\* analyses of the core of zoned zircons.

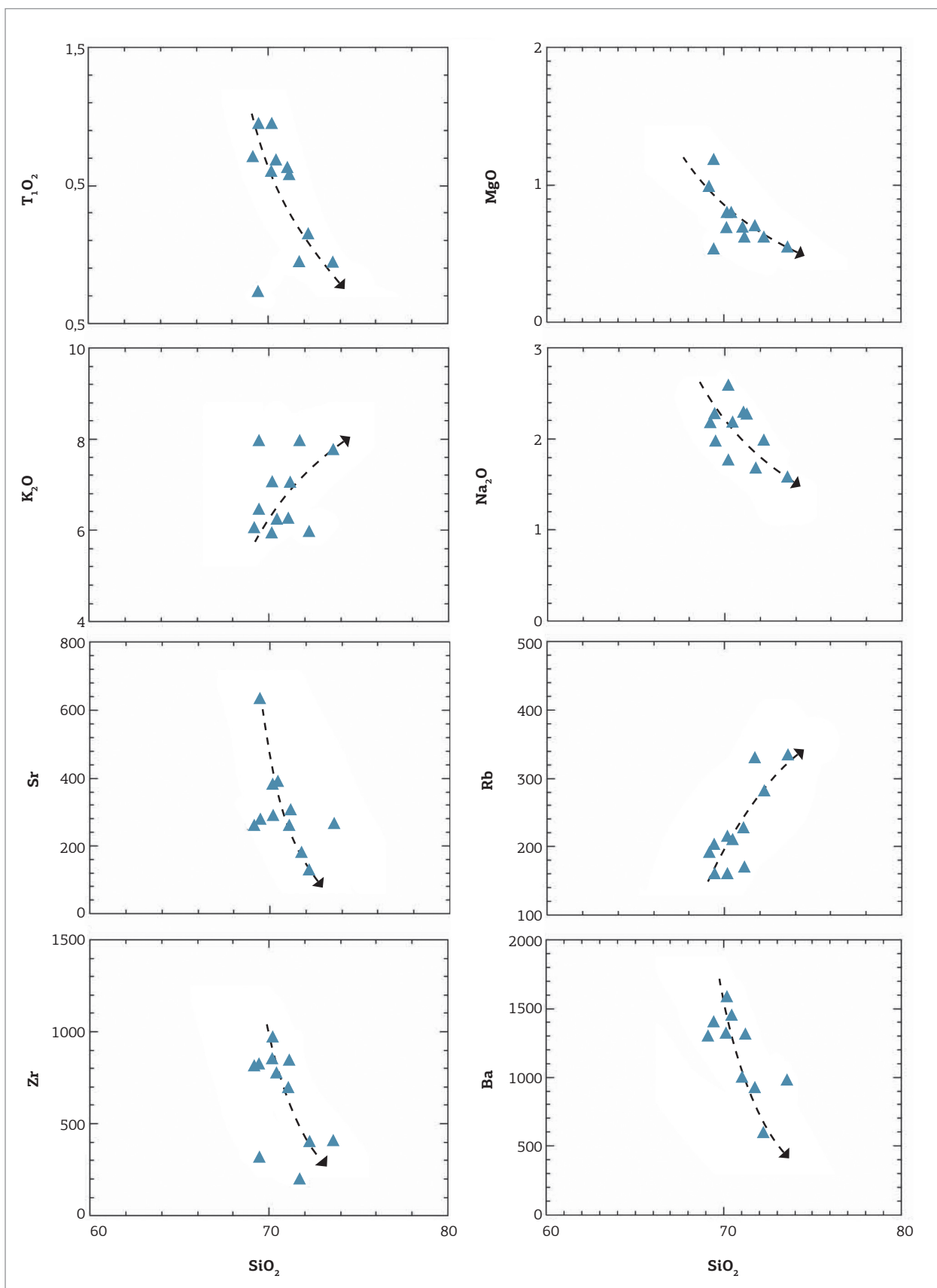


Figure 5. Chemical variation diagrams of Harker (1909) for major and trace elements of the monzo-syenogranitic bodies of Salvador.

and peraluminous, indicating a possible origin from the partial fusion of a crustal source, a hypothesis that is corroborated by the negative values of  $\epsilon_{\text{Nd(t)}}$  (-6.08). The rocks are enriched in LREE and present strong negative Eu anomalies.

The Sm-Nd model age ( $T_{\text{DM}}$ ) around 2.9 Ga seems to indicate a Neoarchean source for these lithotypes. The U-Pb zircon ages of  $2,064 \pm 36$  and  $2,064 \pm 6$  Ma obtained in this study are similar to the U-Pb (SHRIMP) and Pb-Pb (evaporation) zircon ages of the syenites and post-tectonic granites from the ISCB, where ages ranged from 2.06 to 2.09 Ga (Peucat *et al.* 2011 and references therein) (Tab. 1).

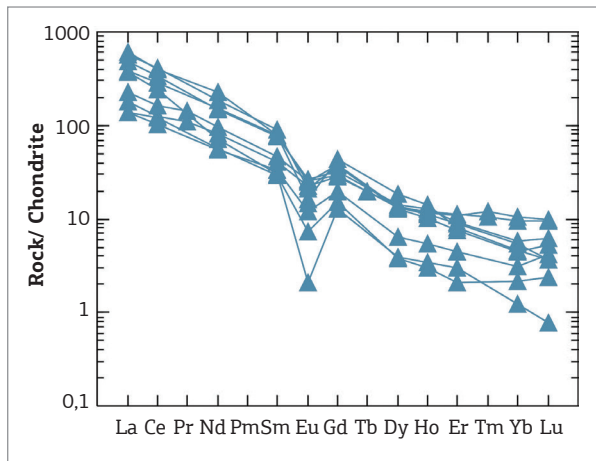


Figure 6. Chondrite-normalized rare earth elements patterns for the monzo-syenogranitic bodies. The chondrite values are from Evensen *et al.* (1978).

On the basis of the present results and the recent studies performed by Souza (2013), the monzo-syenogranites can be positioned as late- to post-tectonic granites, since they exhibit deformation related to the late dextral shear zones dated at  $2,064 \pm 9$  Ma (*in situ* LA-ICPMS monazite) of Paleoproterozoic orogenesis in the SEB.

Moreover, taking into account the age of  $2,083 \pm 4$  Ma attributed to the metamorphism of the ISCB (Peucat *et al.* 2011), the geochemical and geochronological data found in this study are compatible with the geodynamic model proposed by Barbosa and Sabaté (2002, 2004), as well as with the tectonic evolution of the northeastern part of the ISCB proposed by Oliveira *et al.* (2010). Similar to our conclusion, these geodynamic models include some peraluminous types as late-tectonic granites, which are undeformed or rather weakly deformed and cut through the older granulitic rocks and exhibit negative values of  $\epsilon_{\text{Nd(T)}}$  between -13 and -5.

## ACKNOWLEDGMENTS

We wish to acknowledge the financial resources provided by CNPq for the field work, the Doctorate degree grant of the first author by CAPES, and the financial support for the reciprocal visits of the second author in Brazil and of the third author in France at the Université Blaise Pascal (Project No. 624/09) by CAPES-COFECUB. We also acknowledge the financial resources provided for laboratorial work by CBPM and CPRM.

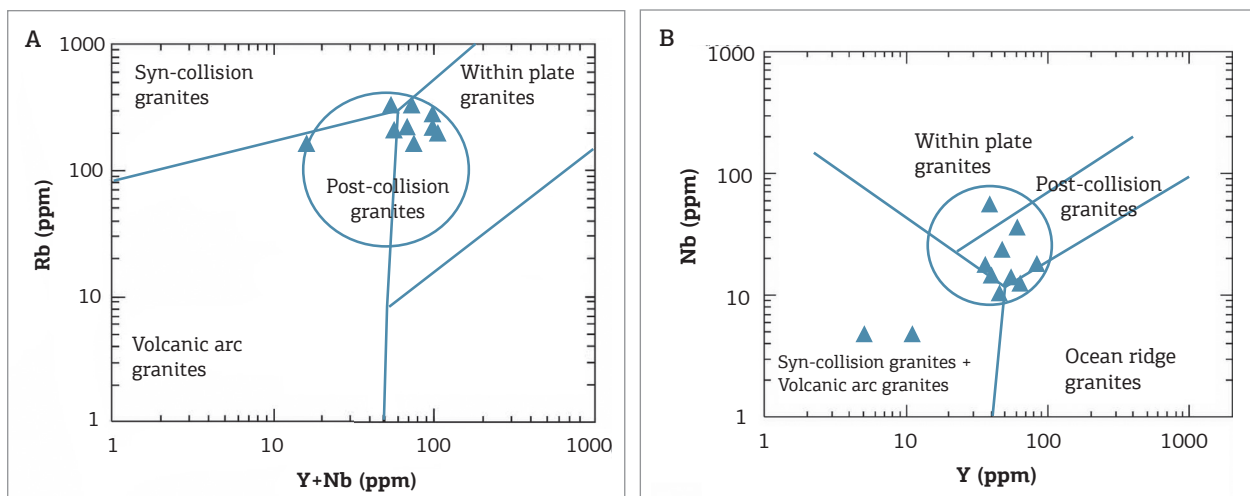


Figure 7. (A) Rb versus (Nb + Y) diagram, discriminating tectonic environments for granites (Pearce *et al.* 1984). (B) Nb versus Y diagram, discriminating tectonic environments for granites (Pearce *et al.* 1984). The ellipse corresponds to the field of post-collision granites of Pearce (1996).

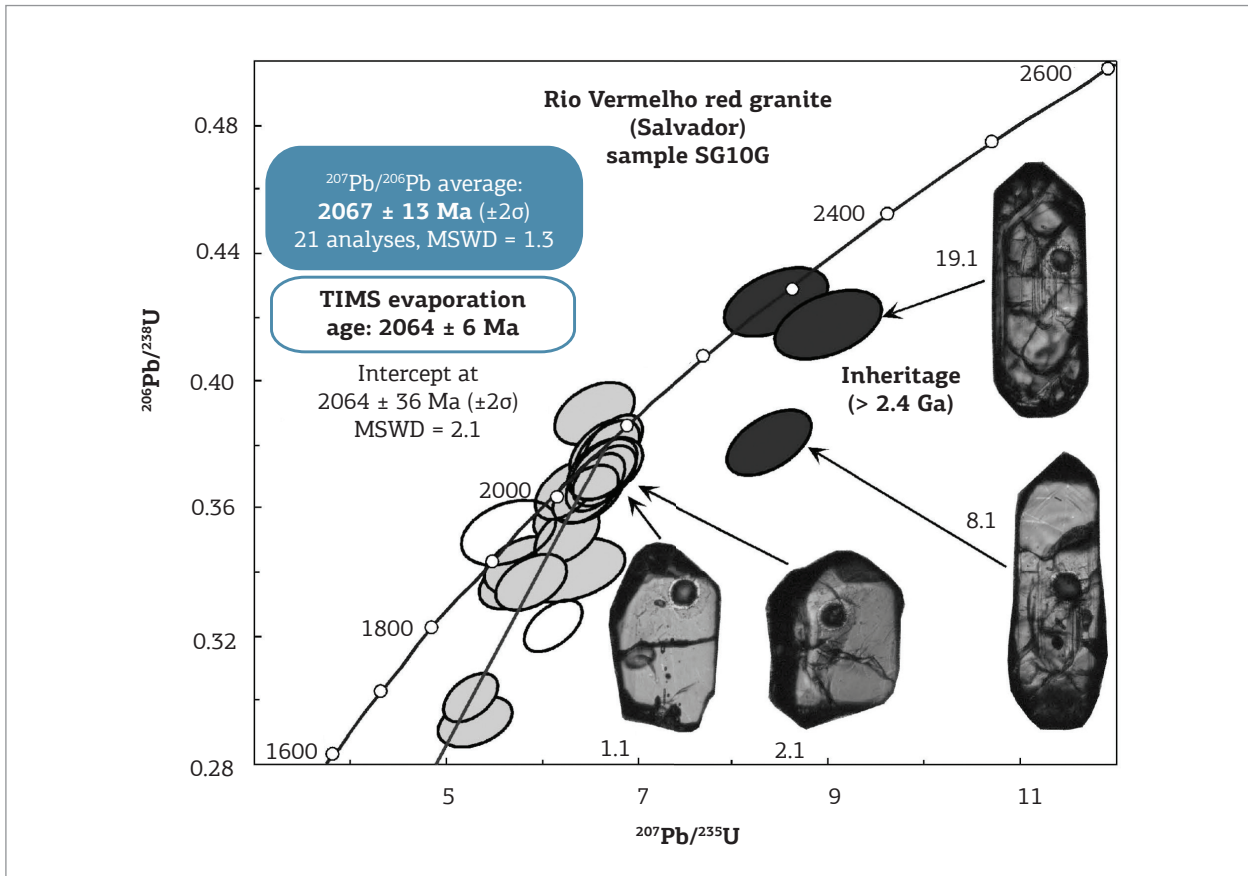


Figure 8. Concordia diagram with U-Pb data in zircon crystals from the SG-10G sample obtained through LA-ICPMS. Images of zircon crystals under transmitted light. The circles correspond to the spots (20  $\mu\text{m}$ ).

## REFERENCES

- Alkmim F.F., Neves B.B.B., Alves J.A.C. 1993. Arcabouço tectônico do Cráton do São Francisco – Uma revisão. In: Dominguez J.M.L. & Misi A. (eds.). *O Cráton do São Francisco*. SBG-NBA/SE, SGM, CNPq, Salvador, p. 45-62.
- Almeida F.F.M. de. 1977. O Cráton do São Francisco. *Revista Brasileira de Geociências*, **7**:349-364.
- Barbosa J.S.F. 1990. The granulites of the Jequié complex and Atlantic mobile belt, southern Bahia, Brazil: an expression of Archean-Proterozoic plate convergence. In: Vielzeuf D. & Vidal P. (eds.), *Granulites and Crustal Evolution*. Springer-Verlag, France, p. 195-221.
- Barbosa J.S.F. & Dominguez J.M.L. (eds.). 1996. *Texto Explicativo para o Mapa Geológico ao Milionésimo*. SICM/SGM, Salvador (Edição Especial), 400 p.
- Barbosa J.S.F. & Sabaté P. 2002. Geological features and the Paleoproterozoic collision of four Archaean Crustal segments of the São Francisco Craton, Bahia, Brazil. A synthesis. *Anais da Academia Brasileira Ciências*, **74**(2):343-359.
- Barbosa J.S.F. & Sabaté P. 2004. Archean and Paleoproterozoic crust of the São Francisco Cráton, Bahia, Brazil: geodynamic features. *Precambrian Research*, **133**:1-27.
- Barbosa J.S.F., Corrêa-Gomes L.C., Dominguez, J.M.L., Cruz S.A.S., Souza, J.S. 2005. Petrografia e Litogeocímica das Rochas da Parte Oeste do alto de Salvador, Bahia. *Revista Brasileira de Geociências*, **35**(4 Supl): 9-22.
- Barbosa J.F.S., Peucat J.J., Martin H., da Silva F.A., de Moraes A.M., Corrêa-Gomes L.C., Sabaté P., Marinho M.M., Fanning C.M.F. 2008. Petrogenesis of the late-orogenic Bravo granite and surrounding high-grade country rocks in the paleoproterozoic orogen of Itabuna-Salvador-Curaçá block, Bahia, Brazil. *Precambrian Research*, **167**: 35-52.
- Celino J.J., Conceição H., Corrêa-Gomes L.C. 1984. Monzogranito porfirítico: magmatismo ácido tardio no Cinturão Granulítico Atlântico, Salvador, Bahia. In: SBG, Congr. Bras. Geol., **33**, Bol. Res., 157-158.
- Chappell, B.W. & White, A.J.R. 1974. Two contrasting granite types. *Pacific Geology*, **8**:173-174.
- Conceição H., Rosa M.L.S., Macambira M.J.B., Scheller T., Marinho M.M., Rios D.C. 2003. 2,09 Ga idade mínima da cristalização do Batólito Sienítico Itiúba: um problema para o posicionamento do clímax do metamorfismo granulítico (2,05-2,08 Ga) no Cinturão Móvel Salvador-Curaçá, Bahia. *Revista Brasileira de Geociências*, **33**(3):395-398.
- Corrêa Gomes L.C., Tanner de Oliveira M.A.F., Motta A.C., Cruz M.J.M. (eds.). 1996. *Província de Diques Máficos do Estado da Bahia Mapa, estágio atual do conhecimento e evolução temporal*. SICM/SGM, Salvador (Edição Especial), 144 p.

- Dalton de Souza J., Kosin M., Melo R.C., Santos R.A., Teixeira L.R., Sampaio A.R., Guimarães J.T., Vieira Bento R., Borges V.P., Martins A.A.M., Arcanjo J.B., Loureiro H.S.C., Angelim L.A.A. 2003. Mapa Geológico do Estado da Bahia – Escala 1:1.000.000. Salvador: CPRM, 2003. Versão 1.1. Programas Carta Geológica do Brasil ao Milionésimo e Levantamentos Geológicos Básicos do Brasil (PLGB). Convênio de Cooperação e Apoio Técnico-Científico CBPM-CPRM.
- Delgado I.M., Souza J.D., Silva L.C., Silveira Filho N.C., Santos R.A., Pedreira A.J., Guimarães J.T., Angelim L.A.A., Vasconcelos A.M., Gomes I.P., Lacerda Filho J.V., Valente C.R., Perrotta M.M., Heineck C.A. 2002. Escudo Atlântico. In: Buzzi L.A., Schobbenhaus C., Vidotti M., Gonçalves J.H. (eds.), *Geologia, Tectônica e Recursos Minerais do Brasil*. texto, mapas & SIG. CPRM – Serviço Geológico do Brasil, Brasília, 692 p.
- Del-Rey Silva L.J.H., Dantas E.T., Teixeira J.B.G., Laux J.H., da Silva M.G. 2007. U-Pb and Sm-Nd geochronology of amphibolites from the Curaçá belt, São Francisco Craton, Brazil: tectonic implications. *Gondwana Research* **12**: 454-467.
- Dominguez J.M.L., Martin L., Bittencourt A.C.S.P., Testa V., Leão Z.M.A.N., Silva C. de C. 1999. *Atlas Geoambiental da Zona Costeira do Estado da Bahia*, Convênio UFBA/SME.
- Druguet E., Czechb D.M., Carreras J., Castaño L.M. 2008. Emplacement and deformation features of syntectonic leucocratic veins from Rainy Lake zone (Western Superior Province, Canada). *Precambrian Research*, **163**:384-400.
- Evensen N.M., Hamilton P.J., O'Nions R.R. 1978. Rare earth abundances in chondritic meteorites. *Geochimica et Cosmochimica Acta*, **42**:1199-1212.
- Figueiredo M.C.H. 1989. Geochemical evolution of eastern Bahia, Brazil: a probable early Proterozoic subduction-related magmatic arc. *Journal of South American Earth Sciences*, **2**:131-145.
- Fujimori S. 1968. Granulitos e charnockitos de Salvador (Ba). *Anais da Academia Brasileira Ciências*, **40**:181-202.
- Fujimori S. 1988. Condições de P-T de formação dos granulitos do Farol da Barra, Salvador, Bahia, Brasil. *Revista Brasileira de Geociências*, **18**:339-344.
- Fujimori S. & Allard G.O. 1966. Ocorrência de safirina em Salvador, Bahia. *Bulletin da Sociedade Brasileira de Geologia*, **15**:67-81.
- Harker A. (ed.) 1909. *The Natural History of Igneous Rocks*. Macmillan Publishers, New York, p. 384.
- Hurai V., Paquette J.L., Huraiová M., Konecny P. 2010. Age of deep crustal magmatic chambers in the intra-Carpathian back-arc basin inferred from LA-ICPMS U-Th-Pb dating of zircon and monazite from igneous xenoliths in alkali basalts. *Journal of Volcanology and Geothermal Research*, **198**:275-287.
- Irvine T.N. & Baragar V.R.A. 1971. A guide to the chemical classification of common volcanic rocks. *Canadian Journal of Earth Sciences*, **8**:523-548.
- Kober B. 1986. Whole-grain evaporation for 207Pb/206Pb age investigations on single zircons using a double-filament thermal ion source. *Contributions to Mineral Petrology*, **93**:482-490.
- Ledru P., Johan V., Milési J.P., Tegyey M., 1994. Markers of the last stages of the paleoproterozoic collision: evidence for a 2 Ga continent involving circum-South Atlantic provinces. *Precambrian Research*, **69**: 169-191.
- Ludwig K.R. 2001. User's manual for Isoplot/Ex, Version 2.49. A geochronological toolkit for Microsoft Excel. Berkeley Geochronology Center. Special Publication 1.
- Melo R.C., Loureiro H.S.C., Pereira L.H.M. 1995. Programa Levantamentos Geológicos Básicos do Brasil. Serrinha. Folha SC-24-Y-D. Escala 1: 250.000. MME/CPRM/SUREG-SA. 80 p.
- Menezes Leal A.B., Corrêa-Gomes L.C., Guimaraes J.T. 2012. Diques Maficos. In: Barbosa J.S.F. (Coordenação Geral). *Geologia da Bahia. Pesquisa e Atualização*. Salvador, Volume 2, p. 199-231.
- Mestrinho S.S.P., Linhares P., Carvalho, I.G. 1988. Geoquímica de elementos principais e traços do dique de diabásio da praia de Ondina, Salvador, Bahia. In: *Congr. Bras. Geol.*, **32**, Anais, **4**:1862-1877.
- Oliveira Junior T.R. 1990. Geologia do extremo nordeste do Cráton do São Francisco, Bahia. Dissertação de Mestrado, Instituto de Geociências, Universidade Federal da Bahia. 126 p.
- Oliveira E.P., Windley B.F., McNaughton N.J., Pimentel M., Fletcher I.R. 2004. Contrasting copper and chromium metallogenic evolution of terranes in the Palaeoproterozoic Itabuna-Salvador-Curacá orogen, São Francisco craton, Brazil: new zircon (SHRIMP) and Sm-Nd (model) ages and their significance for orogen-parallel escape tectonics. *Precambrian Research*, **128**(1-2):143-165.
- Oliveira E.P., McNaughton N.J., Armstrong R. 2010. Mesoarchaean to palaeoproterozoic growth of the northern segment of the Itabuna-Salvador-Curaçá orogen, São Francisco Craton, Brazil. In: Kusky T.M., Zhai M.G., Xiao W. (eds.), *The Evolving Continents: Understanding Processes of Continental Growth*. Geological Society of London, Special Publications, **338**:263-286.
- Pearce J.A. 1996. Sources and settings of granitic rocks. *Episodes*, **19**:120-125.
- Pearce J.A., Harris N.B.W., Tindle A.G. 1984. Trace element discrimination diagrams for the tectonic interpretation of granitic rocks. *Journal of Petrology*, **25**:956-983.
- Peucat J.J., Ménot R.P., Monnier O., Fanning C.M., 1999. The Terre Adélie basement in the East-Antarctica Shield: geological and isotopic evidence for a major 1.7 Ga thermal event: comparison with Gawler craton in South Australia. *Precambrian Research*, **94**:205-224.
- Peucat J.-J., Barbosa J.S.F., Pinho I.C. de A., Paquette J.-L., Martin H., Fanning C.M., Menezes Leal A.B., Cruz S.C.P. 2011. Geochronology of granulites from the south Itabuna-Salvador-Curaçá Block, São Francisco Craton (Brazil): Nd isotopes and U-Pb zircon ages. *Journal of South American Earth Sciences*, **31**:397-413.
- Pupin J.P. 1980. Zircon and granite petrology. Contributions to Mineralogy and Petrology **73**: 207-220.
- Rosa M. de Lda.S., Conceição H., Macambira M.J.B., Scheller T., Martin H., Bastos Leal, L.R. 2001. Idades Pb-Pb e assinatura isotópica Rb-Sr e Sm-Nd do magmatismo sienítico paleoproterozoico no sul do Cinturão Móvel Salvador-Curaçá: Maciço Sienítico de São Felix, Bahia. *Revista Brasileira de Geociências* **31**: 397-400.
- Shand S.J. (ed.). 1950. *Eruptive Rocks Their Genesis, Composition, Classification and Their Relation to Ore Deposit*, 4th edn., Thomas Murby, London, 488 p.
- Silva L.C., McNaughton N.P., Melo R.C., Fletcher I.R. 1997. U-Pb SHRIMP ages in the Itabuna-Caraíba TTG high-grade Complex: the first window beyond the Paleoproterozoic overprint of the eastern Jequié Craton, NE Brazil. In: *International Symposium on Granites and Associated Mineralization (ISGAM)*. Salvador, Abstracts. p. 282-283.
- Silva L.C., Armstrong R., Delgado I.M., Pimentel M., Arcanjo J.B., Melo R.C., Teixeira L.R., Jost H., Cardoso Filho J.M., Pereira L.H.M. 2002. Reavaliação da evolução geológica em terrenos Pré-cambrianos brasileiros com base em novos dados UePb SHRIMP, parte I: Limite centro-oriental do Cráton do São Francisco. *Revista Brasileira de Geociências*, **32**(4):501-502.
- Souza J.S. de. 2013. Geologia, Metamorfismo e Geocronologia de Litotipos de Salvador-Bahia. Tese de Doutorado, Instituto de Geociências, Universidade Federal da Bahia, 153 p.

- Souza J.S. de, Barbosa J.S.F., Correa-Gomes L.C. 2010. Litogeocímica dos granulitos ortoderivados da cidade de Salvador, Bahia. *Revista Brasileira Geociências*, **40**:339-354.
- Steiger R.H. & Jäger E. 1977. Subcommission on geochronology: convention of the use of decay constants in geo- and cosmochronology. *Earth Planetary Science Letters*, **36**:359-362.
- Teixeira L.R. 1997. O Complexo Caraíba e a Suíte São José do Jacuípe no Cinturão Salvador-Curaçá (Bahia, Brasil): petrologia, geoquímica e potencial metalogenético. Tese de Doutorado, Instituto de Geociências, Universidade Federal da Bahia, Salvador, 243 p.
- Walker G.P.L. & Skelhorn R.R. 1966. Some associations of acid and basic igneous rocks. *Earth Science Reviews*, **2**:93-109.
- White A.J.R. & Chappell B.W. 1977. Ultrametamorphism and granitoid genesis. *Tectonophysics*, **43**:7-22.
- Wiebe R.A. 1991. Commingling of contrasted magmas and generation of mafic enclaves in granite rocks. In: Didier J. & Barbarin B. (eds.), *Enclaves and Granite Petrology*. Elsevier, Amsterdam, p. 393-402.

---

Arquivo digital disponível on-line no site [www.sbg.org.br](http://www.sbg.org.br)

---